





TRAPPC1 is essential for the maintenance and differentiation of common myeloid progenitors in mice

Yanan Xu^{1,†} , Zhaoqi Zhang^{1,2,†} , Yang Zhao^{1,†}, Chenxu Zhao^{1,2}, Mingpu Shi^{1,2}, Xue Dong^{1,2}, Jiayu Zhang^{1,2}, Liang Tan³, Lianfeng Zhang^{4,*}  & Yong Zhao^{1,2,5,**} 

Abstract

Myeloid cell development in bone marrow is essential for the maintenance of peripheral immune homeostasis. However, the role of intracellular protein trafficking pathways during myeloid cell differentiation is currently unknown. By mining bioinformatics data, we identify trafficking protein particle complex subunit 1 (TRAPPC1) as continuously upregulated during myeloid cell development. Using inducible ER-TRAPPC1 knockout mice and bone marrow chimeric mouse models, we demonstrate that TRAPPC1 deficiency causes severe monocyte and neutrophil defects, accompanied by a selective decrease in common myeloid progenitors (CMPs) and subsequent cell subsets in bone marrow. TRAPPC1-deleted CMPs differentiate poorly into monocytes and neutrophils *in vivo* and *in vitro*, in addition to exhibiting enhanced endoplasmic reticulum stress and apoptosis via a Ca²⁺-mitochondria-dependent pathway. Cell cycle arrest and senescence of TRAPPC1-deleted CMPs are mediated by the activation of pancreatic endoplasmic reticulum kinase and the upregulation of cyclin-dependent kinase inhibitor p21. This study reveals the essential role of TRAPPC1 in the maintenance and differentiation of CMPs and highlights the significance of protein processing and trafficking processes in myeloid cell development.

Keywords common myeloid progenitors; myeloid cells; monocytes; neutrophils; TRAPPC1

Subject Categories Immunology; Membranes & Trafficking; Stem Cells & Regenerative Medicine

DOI 10.15252/embr.202255503 | Received 27 May 2022 | Revised 14 November 2022 | Accepted 17 November 2022 | Published online 28 November 2022

EMBO Reports (2023) 24: e55503

Introduction

In mammals, myeloid cells recognize and eliminate pathogens and damage-associated components, in addition to initiating and amplifying adaptive immune responses. The normal development of myeloid cells is essential for the maintenance of their homeostasis. In the hierarchical hematopoietic model, hematopoietic stem cells (HSCs, defined in mouse as CD48⁻CD150⁺Lin⁻Sca1⁺CD117⁺) differentiate into multipotent progenitor cells (MPPs). MPPs then differentiate into either CD16/32^{low}CD34⁺ common myeloid progenitors (CMPs) or common lymphoid progenitors (CLPs). CMPs continue to differentiate into monocytes and neutrophils through CD16/32^{high}CD34⁺ granulocyte-macrophage progenitors (GMPs) and other developmental stages (Iwasaki & Akashi, 2007; Mahalingaiah *et al.*, 2018). A number of key transcription factors, such as PU.1, CCAAT enhancer binding protein alpha (C/EBP α), and Ruppel-like factor 5, are essential for the progression of multipotent progenitors to monocytes/macrophages and neutrophils, although they may act in the bone marrow at different development stages (Zhang *et al.*, 1997; Rosenbauer & Tenen, 2007; Shahrin *et al.*, 2016). In addition to the finely tuned genetic regulatory network, epigenetic and metabolic modulations also play important roles in shaping myeloid cell development in the bone marrow (Alvarez-Errico *et al.*, 2015; Karmaus *et al.*, 2017; Zhao *et al.*, 2018). However, the regulatory role of intracellular protein trafficking pathways in bone marrow myeloid cell differentiation remains unknown.

The intracellular protein trafficking network plays an important role in various physiological and pathological processes (Yu & Hughson, 2010; Kim *et al.*, 2016; Bodnar *et al.*, 2020; Cejas *et al.*, 2021). Intracellular trafficking and precise delivery of newly synthesized and sorted proteins in the Golgi/trans-Golgi network compartments to functional cellular destinations, such as

1 State Key Laboratory of Membrane Biology, Institute of Zoology, Chinese Academy of Sciences, Beijing, China

2 Cunjia Medical School, University of Chinese Academy of Sciences, Beijing, China

3 Kidney Transplantation Department, Second Xiangya Hospital of Central South University, Changsha, China

4 Key Laboratory of Human Diseases Comparative Medicine, Ministry of Health, Institute of Laboratory Animal Science, Chinese Academy of Medical Sciences, Peking Union Medical College, Beijing, China

5 Beijing Institute for Stem Cell and Regenerative Medicine, Beijing, China

*Corresponding author. Tel: +(86)10-87778442; E-mail: zhanglf@cnilas.org

**Corresponding author. Tel: +(86)10-64807302; E-mail: zhaoy@ioz.ac.cn

[†]These authors contributed equally to this work

endosomes, lysosomes, and plasma membranes, are crucial to normal cell function (Barlowe & Miller, 2013; Wang *et al.*, 2021). Trafficking protein particle complex subunit 1 (TRAPPC1) is a core subunit of transport protein particle (TRAPP) complexes (Kim *et al.*, 2016). TRAPP complexes, first identified and studied in yeast, are composed of three different complexes sharing the same multicomponent protein core (Sacher *et al.*, 1998, 2001, 2019; Lynch-Day *et al.*, 2010). All of the yeast subunits are conserved in mammals, including humans. TRAPP complexes and their subunits play certain roles in processes related to vesicle traffic, including endoplasmic-reticulum-to-Golgi trafficking and autophagy (Yamasaki *et al.*, 2009; Scrivens *et al.*, 2011; Ramirez-Peinado *et al.*, 2017; Zhao *et al.*, 2017). We recently reported that specific TRAPPC1 deficiency in thymic epithelial cells significantly impairs thymic development in mice (Dong *et al.*, 2022). However, little is currently known about TRAPP complexes in immune cell development. In this study, after observing continuously upregulated levels of protein processing in the endoplasmic reticulum and of TRAPPC1 expression during the HSC-to-CMP-to-GMP developmental transition in bone marrow as analyzed by bioinformatics data mining, we investigated the roles of TRAPPC1 in bone marrow myeloid cell development using established inducible ER-TRAPPC1 knockout mice and chimeric mouse models.

Results

TRAPPC1 is gradually upregulated in the bone marrow during myeloid cell development

To screen signaling pathways or functional genes vital to the process of myeloid cell development, we first analyzed available RNA sequencing (RNA-seq) data (Taiwo *et al.*, 2013; Jeong *et al.*, 2014; Sun *et al.*, 2014) to identify key genes whose transcriptional expression in the bone marrow changes significantly during the development of HSCs to CMPs to GMPs. After defining differentially expressed genes (DEGs, $P < 0.05$, $\log_2|FC| > 2$) for HSCs vs. CMPs and for CMPs vs. GMPs (Fig 1A), Kyoto Encyclopedia of Genes and Genomes (KEGG) analysis showed that endoplasmic reticulum-related pathways, including protein processing in endoplasmic reticulum and protein digestion and absorption, were continuously upregulated during differentiation from HSCs to CMPs to GMPs (Fig 1B; Appendix Fig S1). Gene set enrichment analysis showed that genes involved in protein processing in the endoplasmic reticulum were highly enriched in accordance with developmental phase and were continuously upregulated during myeloid cell development ($P < 0.01$, Fig 1C). A group of genes associated with protein processing in the endoplasmic reticulum was upregulated during the differentiation of CMPs to GMPs (Fig 1D). Several large multisubunit protein complexes are responsible for protein processing in the endoplasmic reticulum; here, we noted that TRAPPC1, a core subunit of the TRAPP complex, was specifically and continuously up-regulated during myeloid precursor development (Fig 1E), which was verified by real-time PCR assays of cells in the CMP differentiation culture system (Fig 1F). These results indicate the potential involvement of protein processing in the endoplasmic reticulum and TRAPPC1 in the differentiation of HSCs to GMPs in bone marrow.

TRAPPC1 is indispensable for myeloid cell development

To study the regulatory roles of TRAPPC1 in myeloid cells, we constructed TRAPPC1-floxed and knockout mice using the CRISPR/Cas9 system (Fig EV1A). Unfortunately, TRAPPC1 KO mice were unattainable due to the fetal lethality of TRAPPC1 deletion (Fig EV1B and C). Therefore, we crossed TRAPPC1-floxed mice with ER^{cre} mice to obtain ER-TRAPPC1 KO mice in which the TRAPPC1 gene can be inducibly knocked out using tamoxifen treatment. To rule out extrinsic interference, we constructed full chimeric mice using lethally irradiated WT CD45.1⁺ recipient mice that received either CD45.2⁺ WT or ER-TRAPPC1 KO BMCs (Appendix Fig S2A). These chimeric mice were then treated with tamoxifen for five consecutive days to delete the TRAPPC1 gene from ER-TRAPPC1 KO BMCs-derived cells. As the half-life period of majority myeloid cells is as short as a few days, a limited time interval between tamoxifen treatment and analysis was beneficial to identifying the direct effect of gene depletion on myeloid cells. After an interval of 3 days, immune cell compositions in the bone marrow, spleen, and peripheral blood were detected by flow cytometry (Appendix Fig S2B, C and D). The results showed that the percentages and cell numbers of Ly6C^{high}CD11b⁺ monocytes and Ly6C^{int}CD11b⁺ neutrophils significantly decreased in the bone marrow, spleen, and peripheral blood of ER-TRAPPC1 KO BMCs to WT full chimeric mice, compared with WT BMCs to WT full chimeric mice (Fig 2A and B; Appendix Fig S3A–C), whereas there was no obvious change in the composition of T and B cells for ER-TRAPPC1 KO chimeras (Fig 2C and D). Furthermore, red blood cell and platelet counts in the peripheral blood were unchanged in these chimeric mice (Fig 2E and F). Mixed WT and ER-TRAPPC1 KO mixed chimeric mice, which received both WT and ER-TRAPPC1 KO BMCs, were used to identify kinetic changes in immune cell subsets across different days after tamoxifen treatment (Appendix Fig S4A–C). The results of flow cytometry analysis showed that monocytes and neutrophils derived from TRAPPC1-deleted BMCs dropped rapidly after tamoxifen treatment, while levels of CD4⁺ T cells, CD8⁺ T cells, and B220⁺ B cells were notably unchanged (Fig 2G; Appendix Fig S5), confirming the specific impact of TRAPPC1 deficiency on myeloid cells. Collectively, these results suggest that TRAPPC1 is indispensable to the myeloid cell development process.

TRAPPC1 deficiency reduces CMPs and impairs development capacity

Survival abnormalities in mature myeloid cells might cause the observed defects in TRAPPC1-deleted mature myeloid cells. Therefore, we detected monocytes and neutrophils in Lyz-TRAPPC1 KO mice, in which TRAPPC1 was deleted during the late developmental stages of monocytes and neutrophils (Clausen *et al.*, 1999). The results showed that the percentages and cell numbers of monocytes and neutrophils were normal in Lyz-TRAPPC1 KO mice compared to WT mice (Appendix Fig S6A–C). In addition, the percentages of Annexin V⁺ and Ki67⁺ cells in TRAPPC1-deleted monocytes and neutrophils were similar to those found in WT cells (Appendix Fig S7A and B), indicating that TRAPPC1 deficiency in mature monocytes/macrophages and neutrophils does not impair their apoptosis or proliferation and suggesting that the decreased presence of monocytes and neutrophils in ER-TRAPPC1 KO BMCs compared to WT

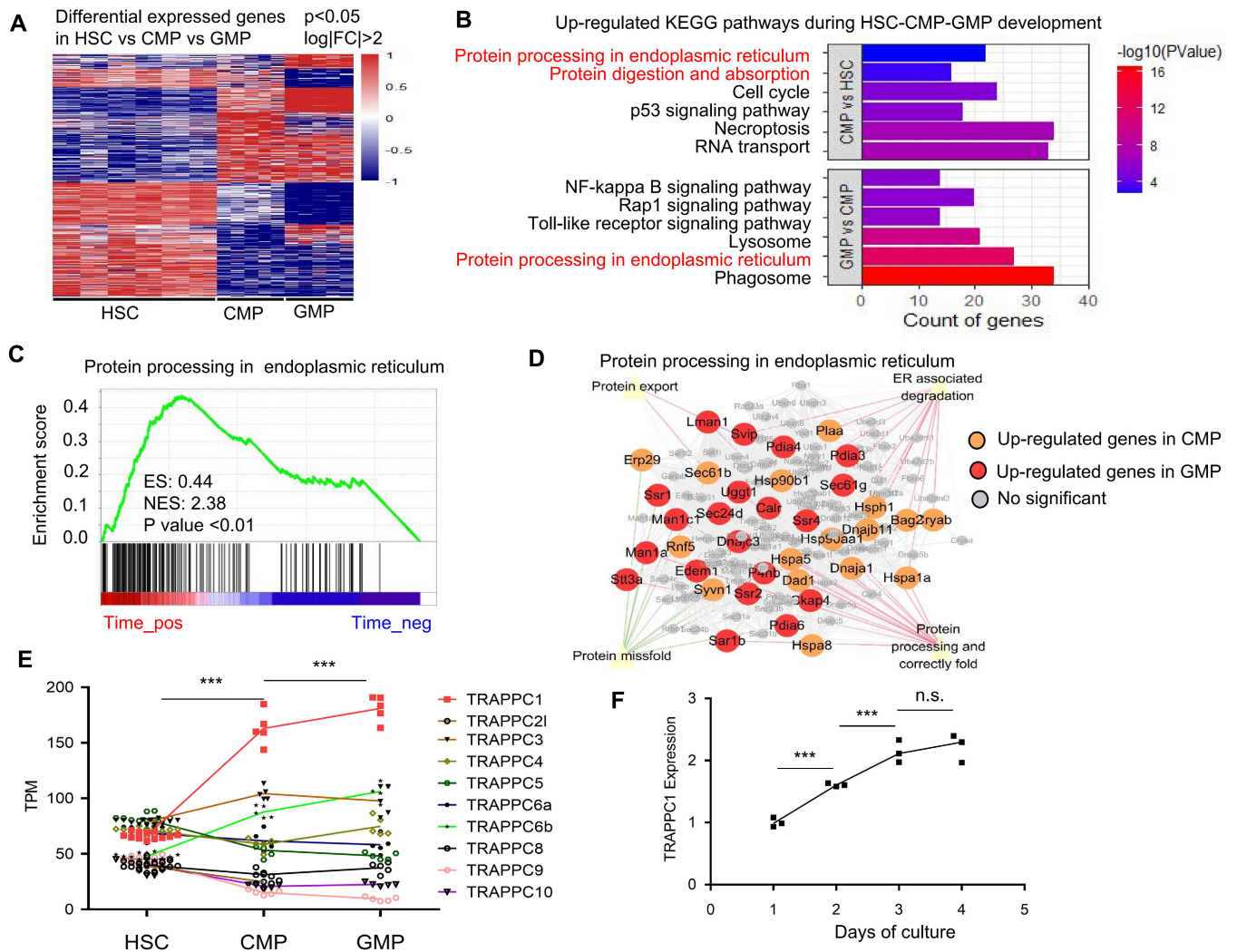


Figure 1. TRAPPC1 is gradually upregulated during myeloid cell development.

A Heat map representing the gene expression profile of HSCs, CMPs, and GMPs, selected genes were from the union set of DEGs ($P < 0.05$, $\log_2|FC| > 2$) of HSCs vs. CMPs and DEGs ($P < 0.05$, $\log_2|FC| > 2$) of CMPs vs. GMPs.

B KEGG signal pathway enrichment of upregulated genes during HSC-to-CMP-to-GMP development.

C Gene set enrichment analysis plot presenting DEGs during HSC-to-CMP and CMP-to-GMP development (time phase) enriched in protein processing in the endoplasmic reticulum pathway, $P < 0.01$.

D Network analysis showing DEGs related to protein processing in the endoplasmic reticulum.

E Expression of Trapp complex family genes during HSC-to-CMP-to-GMP development ($n \geq 5$, biological replicates).

F Sorted CMPs were cultured with SCF (20 ng/ml), GM-CSF (10 ng/ml), G-CSF (20 ng/ml), and M-CSF (20 ng/ml) for 1–4 days, and the expression of TRAPPC1 was detected by real-time-PCR ($n = 3$, biological replicates).

Data information: Data are shown with each replicate staggered. $**P < 0.01$, $***P < 0.001$, and n.s. $P \geq 0.05$; statistical significance was determined with the two-tailed student's t -test.

Source data are available online for this figure.

chimeras is likely unrelated to increased apoptosis or decreased self-renewal in mature monocytes and neutrophils.

We then quantified the levels of hematopoietic stem and progenitor cells in the bone marrow of WT BMCs to WT and of ER-TRAPPC1 KO BMCs to WT full chimeric mice using multicolor flow cytometry 3 days after tamoxifen treatment (Fig EV2A). The proportions of $CD16/32^{low}CD34^+$ CMPs in $Lin^-Sca1^-CD117^+$ cells were significantly increased, but $CD16/32^{high}CD34^+$ GMPs in

$Lin^-Sca1^-CD117^+$ cells were reduced in ER-TRAPPC1 KO BMCs to WT mice compared to WT BMCs to WT mice (Fig 3A and B). However, the cell numbers of CMPs and GMPs were significantly decreased in ER-TRAPPC1 KO BMCs to WT chimeras (Fig 3C). We also found that the percentages of HSCs ($CD48^-CD150^+Lin^-Sca1^+CD117^+$), MPPs ($CD48^+Lin^-Sca1^+CD117^+$), and $L-S^+K^+$ cells ($Lin^-Sca1^+CD117^+$, a heterogeneous population including HSCs and MPPs) were significantly increased in the bone marrow of ER-

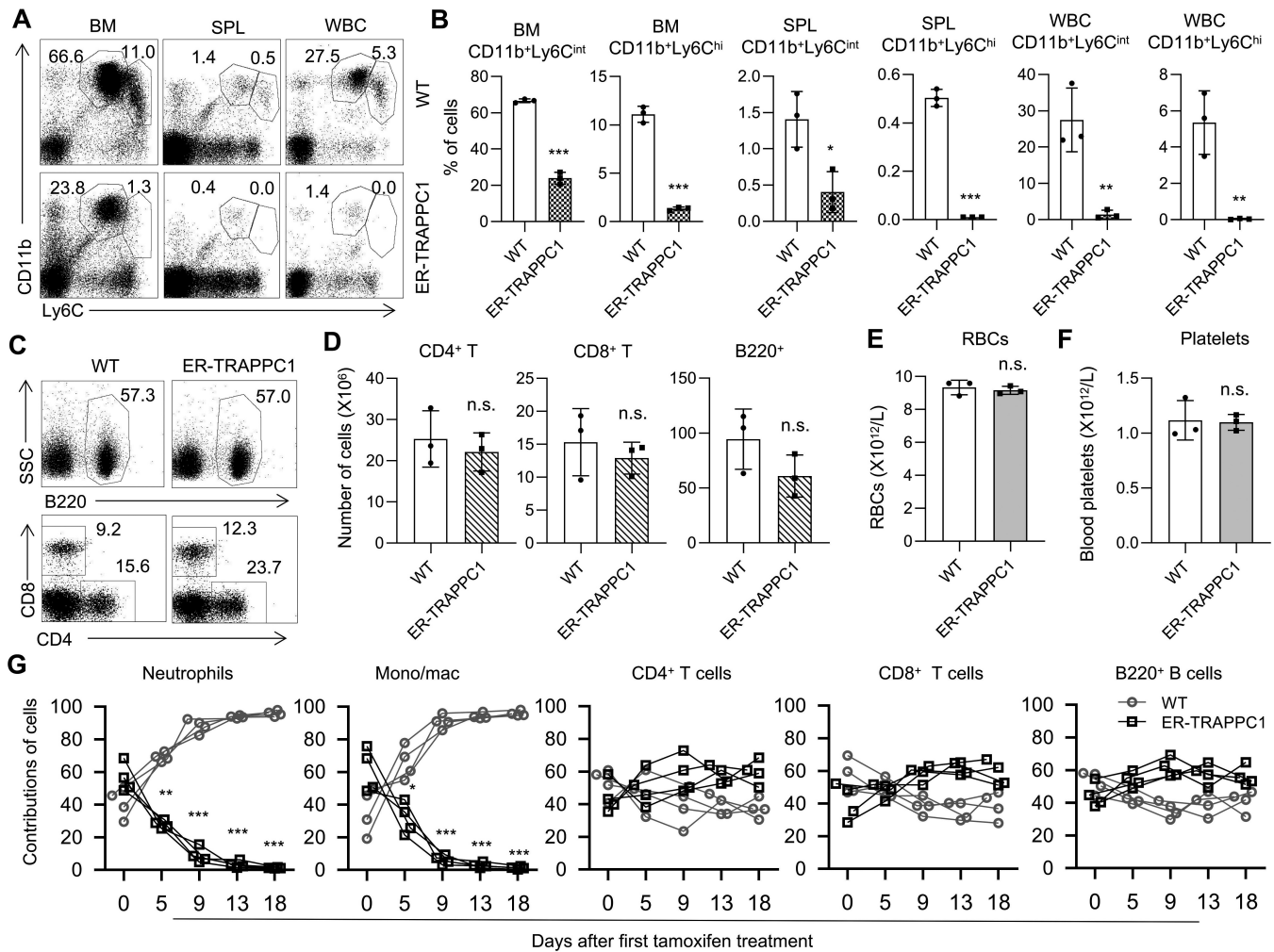


Figure 2. Myeloid cells are severely depleted in ER-TRAPPC1 KO BMCs to WT chimeric mice.

WT and ER-TRAPPC1 BMCs to WT full chimeras were treated by tamoxifen for 5 consecutive days, with an interval of 3 days before flow cytometry analysis of myeloid cells in the bone marrow, spleen, and peripheral blood.

A Representative dot plots.

B Percentages of CD11b⁺ Ly6C^{high} monocytes and CD11b⁺ Ly6C^{int} neutrophils in bone marrow, spleen, and peripheral blood ($n = 3$, biological replicates).

C Representative dot plots of T cells and B cells in spleen samples.

D Cell numbers of T cells and B cells in spleen samples ($n = 3$, biological replicates).

E, F Red blood cell and platelet counts of peripheral blood from WT and ER-TRAPPC1 KO BM chimeras ($n = 3$, biological replicates).

G Mixed WT and ER-TRAPPC1 BMCs to WT chimeras were treated with tamoxifen for 5 consecutive days, and changes in the chimera level of different cell sets were analyzed by flow cytometry ($n = 4$, biological replicates).

Data information: Data are shown as means \pm SD. * $P < 0.05$, ** $P < 0.01$, *** $P < 0.001$, and n.s. $P \geq 0.05$; statistical significance was determined with the two-tailed student's t -test.

Source data are available online for this figure.

TRAPPC1 KO BMCs to WT mice (Fig EV2B and C). However, the numbers of HSCs, MPPs, and L⁻S⁺K⁺ cells were unchanged in ER-TRAPPC1 KO BMCs to WT mice (Fig EV2D). These results suggest that TRAPPC1 deletion predominately impairs the developmental stages of CMPs in the bone marrow, likely retarding the differentiation of CMPs into GMPs.

To further confirm the developmental deficiencies of TRAPPC1-deleted CMPs, we sorted TRAPPC1-deleted or WT CMPs and cultured these cells in methylcellulose medium to perform clone

formation assays. TRAPPC1-deleted CMPs greatly lost their ability to differentiate to monocytes/macrophages or neutrophils in M-CSF or G-CSF systems (Fig 3D–H; Appendix Fig S8A–D). Importantly, after adoptive transfer of the sorted WT or TRAPPC1-deleted L⁻S⁻K⁺ cells into irradiated recipient mice (Appendix Fig S9), much lower contribution rates of the TRAPPC1-deleted L⁻S⁻K⁺ cells-derived monocytes and neutrophils were noted in the bone marrow and peripheral blood of recipient mice compared to WT L⁻S⁻K⁺ cells-derived cells (Fig 3I and J). Taken together, these results verify

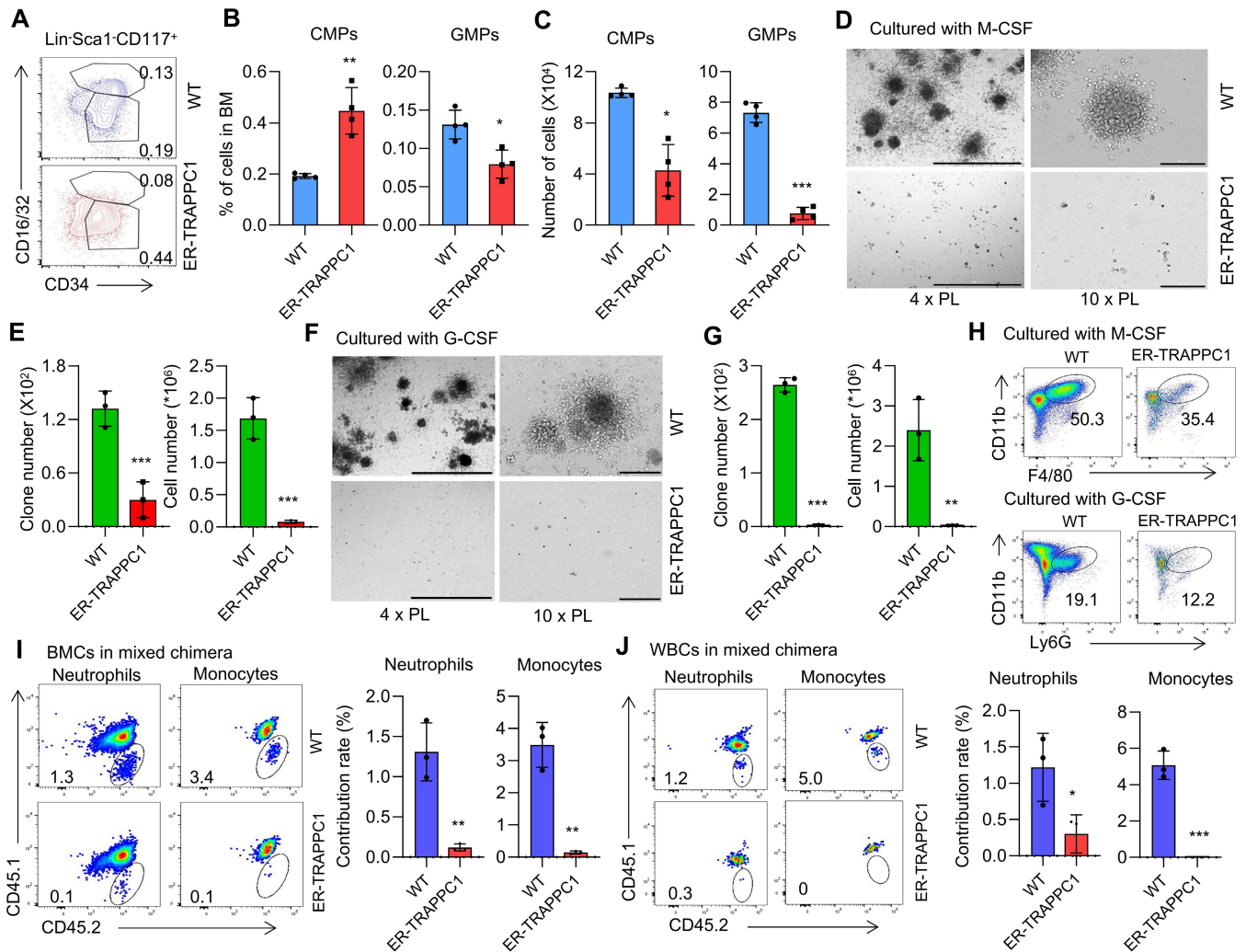


Figure 3. TRAPPC1 deficiency causes a dramatic reduction of CMPs with impaired development capacity.

A–C Flow cytometry analysis of myeloid precursors in BMCs of WT BMCs to WT and ER-TRAPPC1 KO BMCs to WT chimeric mice ($n = 4$, biological replicates). (A) Representative contour diagram of myeloid precursors, including CMPs and GMPs, in WT BMCs to WT and ER-TRAPPC1 KO BMCs to WT chimeric mice. (B) Percentages of CMPs and GMPs in BMCs ($n = 3$, biological replicates). (C) Cell numbers of CMPs and GMPs in bone marrow ($n = 3$, biological replicates). D–H Methylcellulose colony-forming assays of WT and TRAPPC1-deleted CMPs. (D) Representative picture of generated clones after culture with M-CSF, left two (4xPL) with scale bars 1 mm, right two (10xPL) with scale bars 200 μm . (E) Clone numbers and total cell numbers after CMPs were cultured with M-CSF ($n = 3$, biological replicates). (F) Representative picture of generated clones after culture with G-CSF, left two (4xPL) with scale bars 1 mm, right two (10xPL) with scale bars 200 μm . (G) Flow cytometry analysis of generated cells. (H) Clone numbers and total cell numbers after CMPs were cultured with G-CSF ($n = 3$, biological replicates). I, J Sorted CD45.2⁺ WT or ER-TRAPPC1 KO L⁻S⁻K⁺ cells were transferred to CD45.1⁺ recipient mice, and their derived neutrophils and monocytes in WBCs and BMCs were detected at 5 days after transplantation. Contribution analysis of monocytes and neutrophils from donor cells in BMCs (I), and in WBCs (J; $n = 3$, biological replicates).

Data information: Data are shown as mean \pm SD. * $P < 0.05$, ** $P < 0.01$, and *** $P < 0.001$; statistical significance was determined with the two-tailed student's t -test. Source data are available online for this figure.

that TRAPPC1 deficiency severely impairs the differentiation of CMPs into GMPs and, subsequently, into monocytes and neutrophils.

As *in vivo* and *in vitro* development of myeloid cells is highly dependent on colony stimulating factors, including G-CSF, M-CSF, and GM-CSF, we wondered whether the defective development capacity of TRAPPC1 KO CMPs was caused by the interruption of signals from these colony stimulating factors. To this end, these factors' receptors and key downstream transcription factors were

detected in CMPs by quantitative analysis, and the results revealed no significant changes (Appendix Fig S10).

TRAPPC1 deficiency leads to endoplasmic reticulum dysfunction and stress in CMPs

After observing the indispensable role of TRAPPC1 in CMP differentiation into GMPs, we investigated TRAPPC1-regulated pathways by conducting RNA-Seq analysis of the sorted WT and TRAPPC1-

deleted CMPs and GMPs. Analysis of their gene expression profiles suggested that the difference in gene expression between WT and TRAPPC1-deleted CMPs was greater than the difference in gene expression between WT and TRAPPC1-deleted GMPs (Fig 4A; Appendix Fig S11A). Principal component analysis also confirmed that the distance between WT and TRAPPC1-deleted CMPs was significantly farther than that between WT and TRAPPC1-deleted GMPs (Appendix Fig S11B). These results indicate that severely

impaired myeloid cell development after TRAPPC1 deletion might arise from significant changes to CMPs. As the TRAPP complex controls multiple membrane trafficking steps (Yamasaki *et al*, 2009; Scrivens *et al*, 2011; Ramirez-Peinado *et al*, 2017; Zhao *et al*, 2017), we next investigated the endoplasmic reticulum and Golgi of TRAPPC1-deleted CMPs by immunofluorescence assay. The results showed that the endoplasmic-reticulum-to-Golgi intermediate compartment (ERGIC) and Golgi content were significantly decreased in

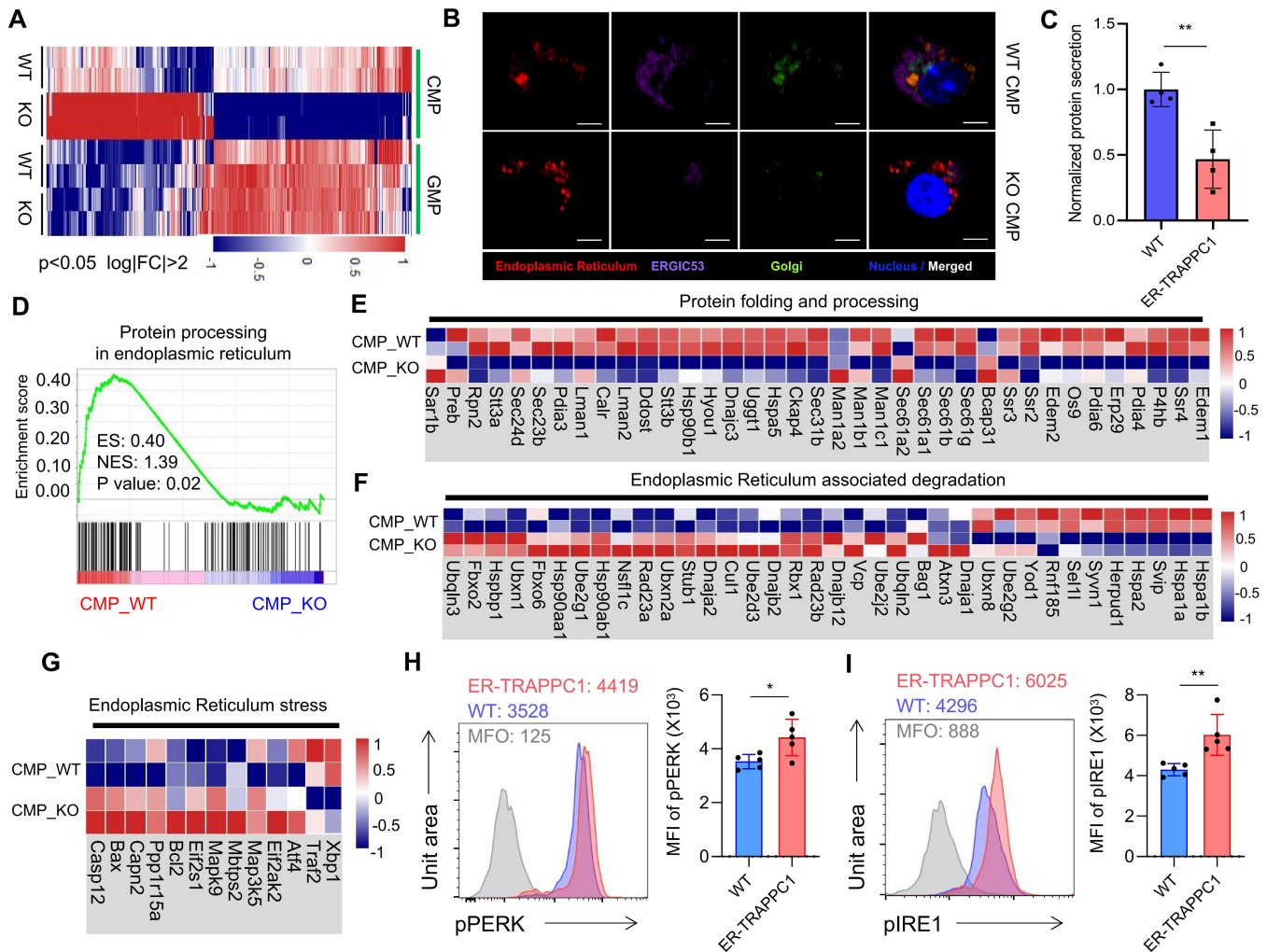


Figure 4. TRAPPC1 deficiency leads to endoplasmic reticulum dysfunction and stress in CMPs.

- A Heat map representing the gene expression profiles of CMPs and GMPs, selected genes were from the union set of DEGs ($P < 0.05$, $\log|FC| > 2$) of WT CMPs vs. TRAPPC1 KO CMPs, and DEGs ($P < 0.05$, $\log|FC| > 2$) of WT GMPs vs. TRAPPC1 KO GMPs.
- B CMPs from WT and ER-TRAPPC1 KO mice were sorted and immuno-stained for Endoplasmic Reticulum (Concanavalin A, red), the endoplasmic-reticulum-to-Golgi intermediate compartment ERGIC (ERGIC53, purple), Golgi (Lectin HPA, green), and nuclei (Hoechst33342, blue). Scale bars, 5 μm .
- C CMPs were sorted and cultured *in vitro* for 24 h, after which total secreted proteins were detected from the supernatant; data were normalized ($n = 4$, biological replicates).
- D Gene set enrichment analysis plot of downregulated DEGs in ER-TRAPPC1 KO CMPs enriched in protein processing in the endoplasmic reticulum pathway, $P = 0.02$.
- E-G Heat map representing upregulated genes ($P < 0.05$) in ER-TRAPPC1 KO CMPs associated with protein folding and processing (E), endoplasmic reticulum-stress (G), and associated degradation (F).
- H, I Intracellular staining of phosphorylated PERK (G, $n = 5$, biological replicates) and phosphorylated IRE1 (H; $n = 5$, biological replicates) in gated WT and ER-TRAPPC1 KO CMPs.

Data information: Data are shown as mean \pm SD. * $P < 0.05$ and ** $P < 0.01$; statistical significance was determined with the two-tailed student's *t*-test. Source data are available online for this figure.

TRAPPC1-deleted CMPs, and we observed a certain degree of endoplasmic reticulum retardation in TRAPPC1-deficient CMPs, indicated by increased fluorescence intensity of the endoplasmic reticulum (Fig 4B; Appendix Fig S12). Transmission electron microscopy of the sorted CMPs also revealed Golgi fragmentation with reduced content in TRAPPC1 KO CMPs (Appendix Fig S13). Along with these changes, the total protein secretion of TRAPPC1 KO CMPs was remarkably lower than that of WT CMPs (Fig 4C). These results imply that TRAPPC1 depletion leads to a certain degree of disorder and dysfunction in the endoplasmic reticulum and Golgi along the secretory pathway. Consistently, gene set enrichment analysis showed that genes related to protein processing in the endoplasmic reticulum were significantly downregulated (Fig 4D). We next conducted an in-depth analysis of endoplasmic reticulum genes and found that most of the genes responsible for protein folding and processing were decreased in TRAPPC1 KO CMPs (Fig 4E). The majority of the genes upregulated in TRAPPC1-deleted CMPs were closely related to endoplasmic reticulum stress and endoplasmic reticulum-associated degradation (Fig 4F and G; Appendix Fig S14), indicating the stressed state of TRAPPC1 KO CMPs. Endoplasmic reticulum perturbations are detected by three endoplasmic reticulum transmembrane protein sensors, inositol requiring enzyme 1 (IRE1), pancreatic endoplasmic reticulum kinase (PERK), and activating transcription factor 6 (ATF6), which respond to endoplasmic reticulum stress and initiate the unfolded protein response (UPR) (Munoz et al, 2013; Tam et al, 2018; Almanza et al, 2019). Therefore, we performed intracellular staining to evaluate the effects of these three protein sensors in WT and TRAPPC1-deleted CMPs. The results showed that phosphorylation levels of PERK and IRE1, denoting the active forms of PERK and IRE1, were significantly upregulated in TRAPPC1-deleted CMPs (Fig 4H and I), whereas expression of the ATF6 protein was unchanged (Appendix Fig S15). Meanwhile, upregulated transcriptional expression of the downstream molecules ATF4, CHOP, and sXBP1 were observed in the sorted WT and TRAPPC1-deleted CMPs by real-time PCR assays, further supporting the activation of PERK and IRE1 pathways in TRAPPC1-deleted CMPs (Fig EV3A). The significantly upregulated protein expression of spliced X-box binding protein 1 (sXBP1) in TRAPPC1-deleted CMPs further confirms the enhanced activation of the IRE1 pathway (Fig EV3B). Overall, these results suggest that TRAPPC1 deficiency in CMPs leads to endoplasmic reticulum dysfunction and stress that promotes UPR and activates PERK- and IRE1-related pathways.

Endoplasmic reticulum stress-induced apoptosis of TRAPPC1-deficient CMPs

We next asked how the endoplasmic reticulum stress caused by TRAPPC1 deletion impedes CMPs differentiation. Transmission electron microscopy was performed on the sorted CMPs, and the results showed that endoplasmic reticulum dilation was significantly augmented in TRAPPC1-deleted CMPs (Fig 5A), consistent with the significantly increased intensity of the fluorescent endoplasmic reticulum tracker observed in TRAPPC1-deleted CMPs by flow cytometry (Fig 5B) and immunofluorescence assay (Fig 4B) and further confirming a considerable degree of endoplasmic reticulum stress in TRAPPC1-deficient CMPs. It is known that irreparable endoplasmic reticulum stress-mediated UPR pathways induce pro-death mechanisms (Maurel et al, 2015). We thus investigated

whether TRAPPC1-deleted CMPs are more susceptible to apoptosis. Both gene set enrichment analysis ($P = 0.01$, Fig 5C) and Annexin V staining (Fig 5D) showed significantly elevated levels of apoptosis in TRAPPC1-deleted CMPs compared to WT CMPs. Increased levels of cleaved-caspase 3 detected by intracellular staining (Fig 5E) suggest that TRAPPC1 deficiency induces apoptosis in CMPs via a caspase-dependent pathway. Autophagy has become recognized as an essential protective mechanism during endoplasmic reticulum stress (Rashid et al, 2015). Thus, we assessed autophagy in CMPs using flow cytometry and observed decreased autophagy in TRAPPC1-depleted CMPs (Appendix Fig S16). Because the PERK/ATF4/CHOP signaling axis plays well-known roles in the induction of apoptosis (Hirsch et al, 2014; Iurlaro & Munoz-Pinedo, 2016), and because we had already verified the increased activation of this signaling axis in TRAPPC1-deleted CMPs (Fig 4H, Fig EV3A), we next evaluated CHOP protein levels using flow cytometry. The results showed that basal CHOP expression in WT CMPs was quite low compared to the fluorescein minus one control (MFO) but was significantly upregulated in TRAPPC1-deleted CMPs (Fig 5F). These results suggest that TRAPPC1 depletion leads to endoplasmic reticulum stress-induced apoptosis through the PERK/CHOP caspase-dependent pathway. To further prove the destructive effects of endoplasmic reticulum stress on myeloid differentiation, we induced endoplasmic reticulum stress in an *in vitro* CMP differentiation system using the endoplasmic reticulum stress inducer thapsigargin. The results showed that thapsigargin significantly blocked differentiation of CMPs into macrophages and neutrophils *in vitro* (Fig 5G and H). Taken together, these results indicate that TRAPPC1 deficiency induces irreparable endoplasmic reticulum stress and results in the apoptosis and defective development of CMPs.

TRAPPC1 deficiency in CMPs causes apoptosis through an endoplasmic reticulum stress-Ca²⁺-mitochondria-dependent pathway

We next sought to gain insight into the mechanism of apoptosis caused by TRAPPC1 depletion. It is well known that endoplasmic reticulum stress is always accompanied by disturbance of intracellular Ca²⁺ homeostasis, which further promotes cell death through apoptosis (Krebs et al, 2015; Bahar et al, 2016). We monitored changes to cytosolic and mitochondrial Ca²⁺ in CMPs using Fluo-4 AM and Rhod-2 AM, respectively. Both cytosolic Ca²⁺ and mitochondrial Ca²⁺ levels were further enhanced in TRAPPC1-deleted CMPs compared to WT CMPs (Fig 6A and B), indicating the dysregulation of Ca²⁺ in TRAPPC1-deleted CMPs. Reactive oxygen (ROS) is another important player in the endoplasmic reticulum stress and apoptosis process (Shen et al, 2014; Kamiya et al, 2018). The intracellular ROS content of TRAPPC1-deleted CMPs was consistently and significantly higher than that of WT CMPs (Fig 6C). Mitochondrial Ca²⁺ overload or oxidative stress will eventually result in the breakdown of mitochondrial membrane potential to cause mitochondrial depolarization, a hallmark of the endogenous apoptosis initiation process (Gonzalez et al, 2010). Mitochondrion swelling was observed in TRAPPC1-deleted CMPs by transmission electron microscopy, revealing an increased size and modest dilution of the matrix, as evidenced by reduced density (Fig 6D). Elevated Mitotracker fluorescence was consistently observed in TRAPPC1-deleted CMPs (Appendix Fig S17). Furthermore, increased proportions of

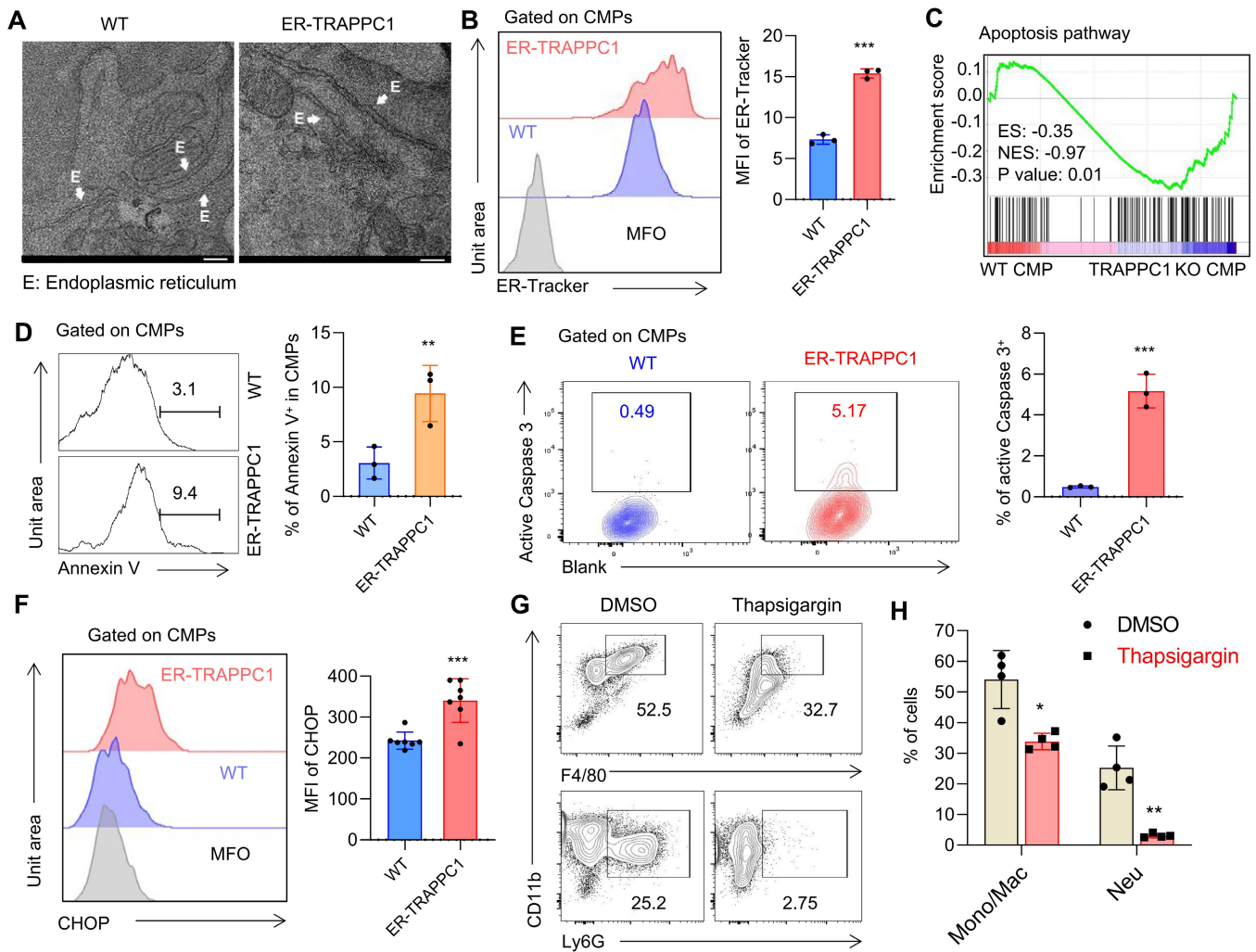


Figure 5. Endoplasmic reticulum stress induces apoptosis of TRAPPC1-deficient CMPs.

A Transmission electron microscopy photograph of sorted CMPs from WT and ER-TRAPPC1 KO mice. Arrows indicate the endoplasmic reticulum. Scale bar, 200 nm.
B Sample of endoplasmic reticulum tracker compared with fluorescence minus one (FMO) and merged mean fluorescence intensity, gated on CMPs ($n = 3$, biological replicates).
C Gene set enrichment analysis plot of up-regulated DEGs in TRAPPC1 KO CMPs enriched in apoptosis pathway, $P = 0.01$.
D Representative histogram and quantification of Annexin V staining of CMPs ($n = 3$, biological replicates).
E Intracellular staining of active caspase 3 in gated CMPs ($n = 3$, biological replicates).
F Intracellular staining of CHOP in gated CMPs ($n = 7$, biological replicates).
G, H Sorted WT CMPs were cultured with SCF (20 ng/ml), GM-CSF (10 ng/ml), G-CSF (20 ng/ml), and M-CSF (20 ng/ml) in the presence of thapsigargin (200 nM) or DMSO for 5 days, then analyzed by flow cytometry ($n = 3$, biological replicates).

Data information: Data are shown as mean \pm SD. * $P < 0.05$, ** $P < 0.01$, and *** $P < 0.001$; statistical significance was determined with the two-tailed student's t -test. Source data are available online for this figure.

cells with low mitochondrial membrane potential were detected in TRAPPC1-deleted CMPs (Fig 6E), suggesting the general loss of mitochondrial membrane potential. To assess mitochondrial membrane permeability, we carried out Cytochrome C (Cyt C) leakage experiments by comparing intracellular Cyt C content after digitonin treatment to content without treatment (Dang et al, 2017). The results revealed the preferential loss of Cyt C in TRAPPC1-deleted CMPs (Fig 6F), indicating higher mitochondrial membrane permeability in TRAPPC1-deleted CMPs. To recapitulate the involvement of endoplasmic reticulum stress and intracellular Ca^{2+} disturbance

in the increased apoptosis of TRAPPC1-deleted CMPs, we evaluated the rescue effect of the endoplasmic reticulum stress inhibitor Tauroursodeoxycholic Acid (TUDCA), which is known to inhibit calcium efflux (Xie et al, 2002). The addition of TUDCA significantly rescued the elevated apoptosis of TRAPPC1-deleted CMPs *in vitro* (Fig 6G). These data indicate that TRAPPC1 deficiency in CMPs causes apoptosis through an endoplasmic reticulum stress- Ca^{2+} -mitochondria-dependent pathway.

As TRAPPC1 deficiency failed to promote apoptosis in mature monocytes or neutrophils (Appendix Fig S7A), we focused on

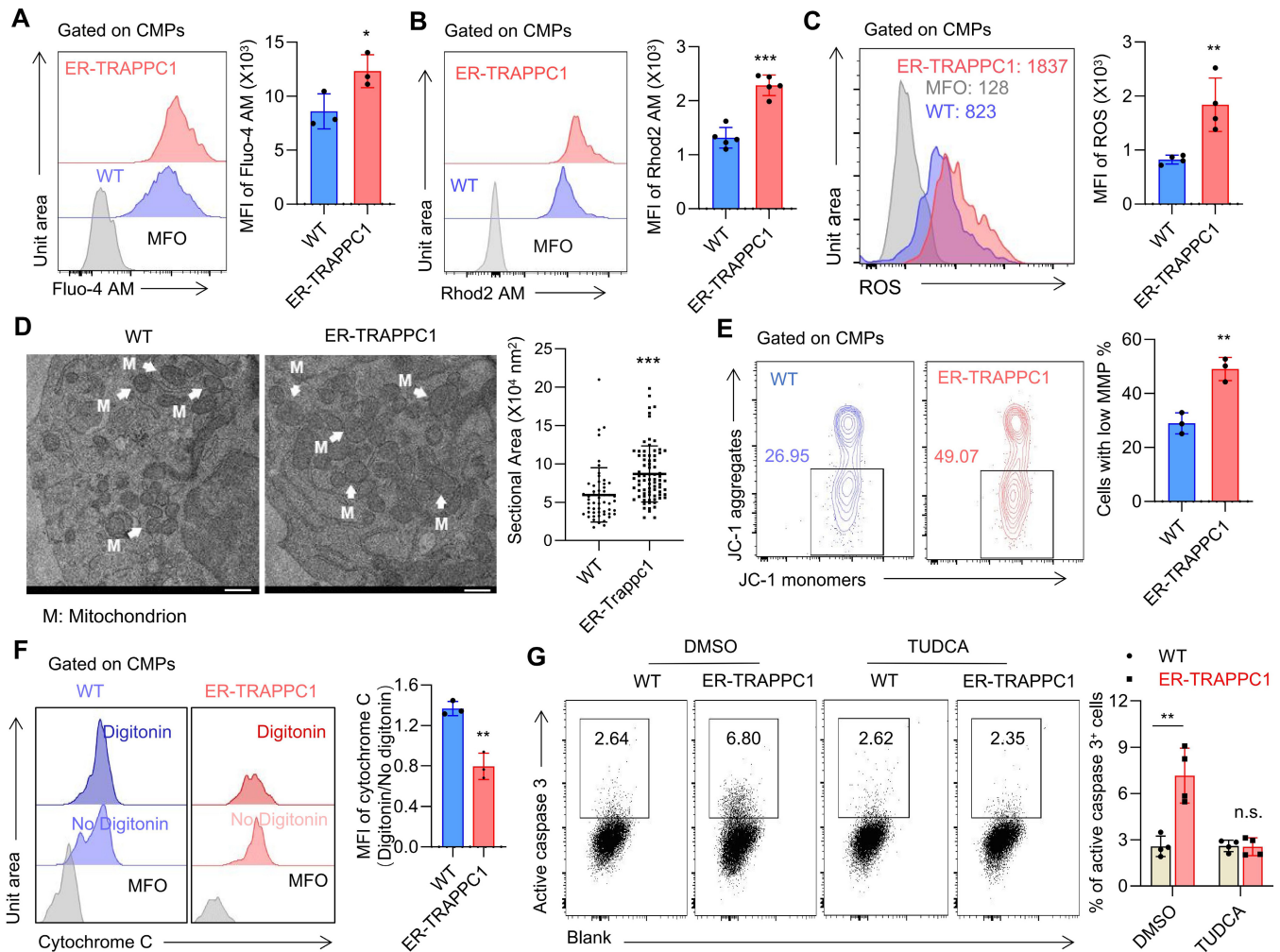


Figure 6. TRAPPC1 deficiency causes apoptosis through an endoplasmic reticulum stress-Ca²⁺ mitochondria-dependent pathway.

A, B Live cell Ca²⁺ detection using the specific indicators Fluo-4 AM for cytosolic Ca²⁺ content detection (A, *n* = 3, biological replicates) and Rhod2 AM for mitochondrial Ca²⁺ content detection (B, *n* = 5, biological replicates).
C Representative overlaid histogram and quantification of cellular reactive oxygen species (ROS), gated on CMPs (*n* = 4, biological replicates).
D Mitochondrial morphology and sectional area calculation under an electron microscope, with arrows indicating the mitochondria. Scale bar, 500 nm (*n* ≥ 50, technical replicates).
E Mitochondrial membrane potential levels of CMPs as evaluated by JC-1 assay. Cells with low mitochondrial membrane potential were quantified, gated on CMPs (*n* = 3, biological replicates).
F Representative histograms and summary graph of intracellular Cyt C staining of CMPs, either permeabilized with digitonin or not (*n* = 3, biological replicates).
G Sorted WT and TRAPPC1-deleted CMPs were cultured with SCF (20 ng/ml), GM-CSF (10 ng/ml), G-CSF (20 ng/ml), and M-CSF (20 ng/ml) in the presence of TUDCA (100 μM) or DMSO for 2 days, then analyzed by flow cytometry (*n* = 3, biological replicates).

Data information: Data are shown as mean ± SD. **P* < 0.05, ***P* < 0.01, ****P* < 0.001, and n.s. *P* ≥ 0.05; statistical significance was determined with the two-tailed student's *t*-test.

Source data are available online for this figure.

exploring the impact of TRAPPC1 deficiency on CMPs. In the myeloid cell development process, CMPs undergo rapid proliferation, whereas mature functional monocytes/macrophages and neutrophils hardly proliferate at all (Rosenbauer & Tenen, 2007). We speculated that the different effect of TRAPPC1 depletion on CMPs compared to monocytes or neutrophils was related to cellular proliferation status. CMP proliferation is strongly dependent on the addition of cytokines (SCF, IL-3, etc.) *in vitro*, and TRAPPC1 deficiency significantly increased CMP apoptosis in this

culture system. However, when we deprived cells of these cytokines to interrupt proliferation, we found that the apoptosis level of TRAPPC1 KO CMPs was quite similar to that of WT CMPs. In addition, upon stopping cell proliferation by preincubation with the proliferation inhibitor Mitomycin C, the apoptosis levels of TRAPPC1 KO CMPs remained similar to those of WT CMPs (Appendix Fig S18A and B). Together, these data imply that TRAPPC1 deficiency tends to induce apoptosis in cells with high proliferative activity.

TRAPPC1 deficiency in CMPs causes cell cycle arrest and senescence by upregulation of p21

Efficient proliferation of myeloid precursors plays a central role in guiding myeloid cell development and homeostasis. The results of an *in vivo* 5-ethynyl-2'-deoxyuridine (EdU) incorporation assay showed that TRAPPC1-deleted CMPs exhibit significantly decreased EdU incorporation (Fig 7A). Cell-cycle analysis of CMPs showed that

TRAPPC1 depletion decreases the proportion of time spent in G1 and S phases while increasing the time spent in G0 phase (Fig 7B and C), suggesting a G0-to-G1 phase arrest in TRAPPC1-deleted CMPs. To identify the key molecules responsible for cell cycle arrest in TRAPPC1-deleted CMPs, we detected expression of cyclins and cyclin-dependent kinases (CDKs), but did not find any detectable defects in the expression of these genes in TRAPPC1-deleted CMPs (Appendix Fig S19A and B). However, we observed significantly

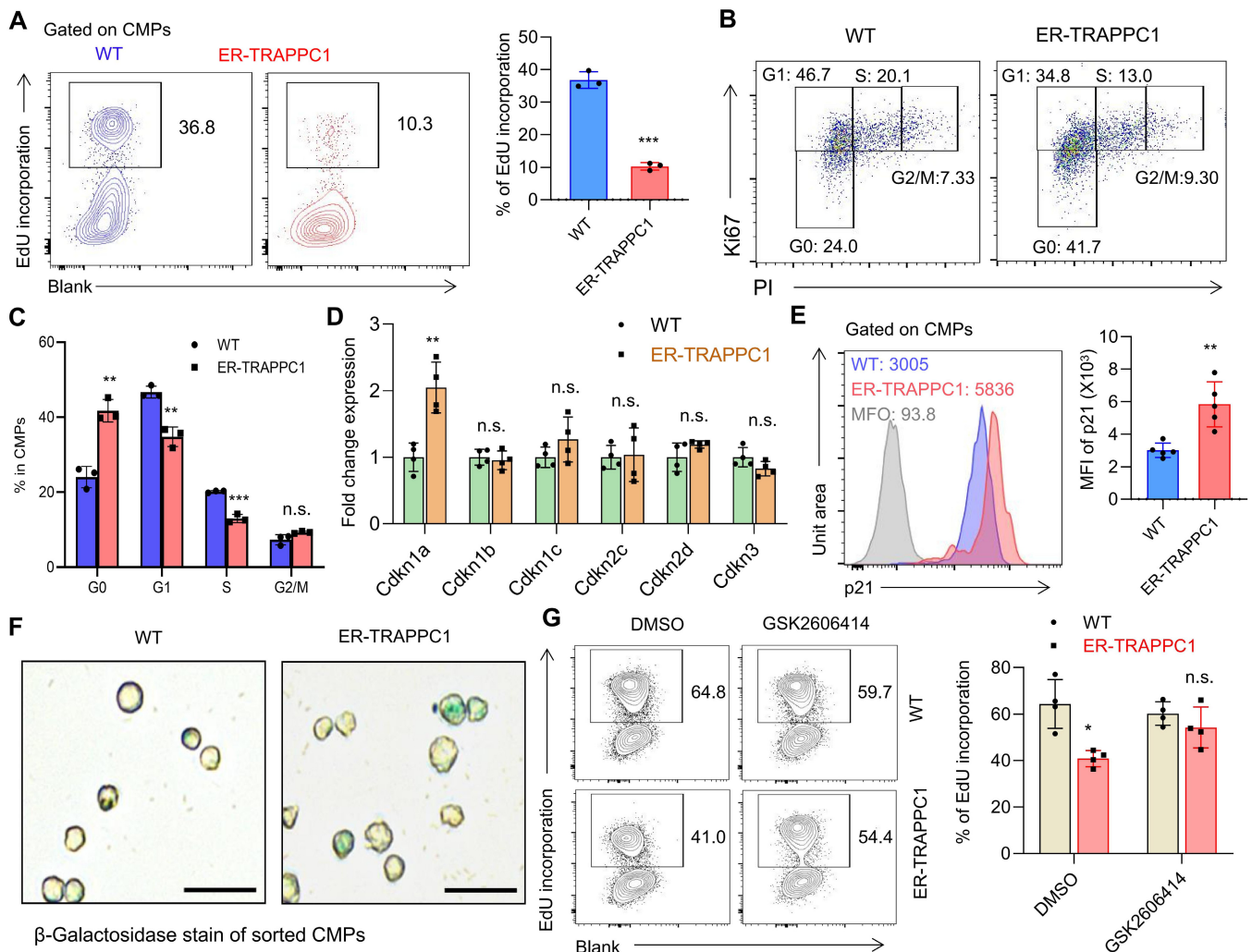


Figure 7. TRAPPC1 deficiency causes cell cycle arrest and senescence by upregulation of p21.

- A 5-ethynyl-2'-deoxyuridine (EdU) incorporation assay of CMPs. Twelve hours before sacrifice, mice were intravenously injected with 1 mg 5-ethynyl-2'-deoxyuridine (EdU) dissolved in PBS. Gated on CMPs ($n = 3$, biological replicates).
- B, C BMCs were stained with antibodies and propidium iodide and assayed for DNA content by flow cytometry, gated on CMPs. (B) Representative dot plot showing G0, G1, S, and G2/M cell cycle phase. (C) Statistical chart ($n = 3$, biological replicates).
- D Normalized gene expression by sorted CMPs ($n = 4$, technical replicates).
- E Intracellular staining of p21 in gated CMPs ($n = 5$, biological replicates).
- F Sorted CMPs were stained with a senescence β -Galactosidase staining kit, and a representative image is shown. Scale bar, 50 μ m.
- G Sorted WT and TRAPPC1-deleted CMPs were cultured with SCF (20 ng/ml), GM-CSF (10 ng/ml), G-CSF (20 ng/ml), and M-CSF (20 ng/ml) in the presence of the PERK inhibitor GSK2606414 (5 nM) or DMSO for 2 days. EdU (10 μ M) was added 12 h before cell harvesting, and cells were analyzed by flow cytometry ($n = 4$, biological replicates).

Data information: Data are shown as mean \pm SD. * $P < 0.05$, ** $P < 0.01$, *** $P < 0.001$, and n.s. $P \geq 0.05$; statistical significance was determined with the two-tailed student's *t*-test.

Source data are available online for this figure.

increased expression of the cyclin-dependent kinase inhibitor gene *cdkn1a*, which encodes p21 (Fig 7D). Consistent with its transcriptional level, p21 protein expression was also elevated in TRAPPC1-deleted CMPs, as evaluated by flow cytometry analysis (Fig 7E). In addition to contributing to cell cycle arrest, p21 can also induce senescence-like changes in murine cells (Chen *et al*, 2002; Hsu *et al*, 2019). Therefore, we were interested in determining whether the cell cycle arrest of TRAPPC1-deleted CMPs was accompanied by cellular senescence. The proportion of positive β -Galactosidase-stained cells increased in TRAPPC1-deleted CMPs, indicating an enhancement of senescence-like changes (Fig 7F). p21 expression is critically regulated by the PERK/CHOP pathway (Mihailidou *et al*, 2010; Rozpedek *et al*, 2016), which is significantly activated in TRAPPC1-deleted CMPs (Figs 4H and 5F, and EV3A). Hence, we performed an *in vitro* rescue experiment using the PERK inhibitor GSK2606414. These results showed that PERK inhibition rescues the defective proliferation of TRAPPC1-deleted CMPs (Fig 7G). These results suggest that TRAPPC1 deficiency in CMPs causes cell cycle arrest and senescence via the PERK-p21 pathway.

We further observed that both TRAPP complex II and TRAPP complex III seemed to persist, in part with incomplete integrity, in TRAPPC1-deficient CMPs across our analysis time frame, as determined by gel filtration (Fig EV4A and B). These findings suggested that TRAPPC1 might contribute to the stability of TRAPP complexes. Using electroporation-delivered small interference RNA (si-RNA), we knocked down other two TRAPP complex subunits in CMPs (Fig EV5A and E), then further assessed their development capacity and gene expression changes. The results indicated that the loss of TRAPPC3 and TRAPPC9 causes obvious development abnormalities (Fig EV5B, C, F, and G) and similar gene expression changes (Fig EV5D and H), including the upregulation of genes related to endoplasmic reticulum stress and cell cycle arrest.

Discussion

After applying bioinformatic methods to outline the key functional genes and pathways involved in the development of myeloid cells in bone marrow, we identified TRAPPC1 as an important “master regulator” gene for CMP development in the bone marrow. Both *in vivo* and *in vitro* experiments illustrated that TRAPPC1 deletion causes a remarkable developmental defect in CMPs, highlighting the indispensability of TRAPPC1 for CMP-to-GMP differentiation. Mechanistic studies revealed that TRAPPC1 deficiency leads to irreparable endoplasmic reticulum stress in CMPs, resulting in the enhancement of apoptosis via a Ca^{2+} -mitochondria-dependent pathway and cell cycle arrest with cellular senescence via upregulation of the p21 pathway.

Hematopoietic stem cells differentiate into MPPs and, subsequently, into CMPs or CLPs. CMPs continue to differentiate into myeloid cells, such as monocytes and neutrophils (Mahalingaiah *et al*, 2018). By using an inducible knockout strategy, we identified a selective defect of monocytes and neutrophils with no detectable changes to T cells, B cells, red blood cells, and platelets in full or mixed ER-TRAPPC1 KO BMCs to WT chimeric mice after short-duration tamoxifen treatment (3–5 consecutive days). After analyzing hematopoietic stem and progenitor cells in the bone marrow of full or mixed chimeric mice, we observed a significant decrease in

the cell numbers of myeloid progenitors CMPs and GMPs in TRAPPC1-deleted BMCs, whereas numbers of MPPs and HSCs remained at levels comparable to WT bone marrow. These results indicate that TRAPPC1 deficiency causes poor CMP survival and blocks the differentiation of CMPs into GMPs *in vivo*. Consistent with these *in vivo* observations, the differentiation ability of TRAPPC1-deleted CMPs was obviously impaired in *in vitro* M-CSF or G-CSF-inducing culture systems, as evidenced by colony formation, cell numbers, and percentages of $\text{CD11b}^+\text{F4}/80^+$ macrophages and $\text{CD11b}^+\text{Ly6G}^+$ neutrophils. Thus, CMPs are more sensitive to TRAPPC1 deficiency than other hematopoietic stem and progenitor cells in the bone marrow; that is, TRAPPC1 is highly critical for the CMP stage of development. The importance of TRAPPC1 in CMPs is further supported by the significantly upregulation of protein processing pathways and TRAPPC1 expression during the differentiation of HSCs into CMPs, as evidenced by RNA-seq assays.

As the largest organelle in the cell, the endoplasmic reticulum plays many important roles, including calcium storage, protein synthesis, and lipid metabolism, and is closely involved in many physiological and pathological progress (Flodby *et al*, 2016; Lee *et al*, 2016; Schwarz & Blower, 2016; Mohamed *et al*, 2020; Xu *et al*, 2020). Both endoplasmic reticulum retardation and fragmentation and content loss of the Golgi complex were observed in TRAPPC1 KO CMPs, and protein synthesis was decreased as well. These findings suggest that TRAPPC1 deficiency causes structural disorder and dysfunction in the endoplasmic reticulum and Golgi components of the secretory pathway. Significant endoplasmic reticulum stress was also strongly demonstrated in TRAPPC1-deleted CMPs through subcellular microscopy, flow cytometry analysis, and quantitative PCR assays, in addition to being observed in TRAPPC1-deleted thymic epithelial cells (Dong *et al*, 2022). This consistency confirms the fundamental importance of TRAPPC1 to endoplasmic reticulum homeostasis across different mammalian cells.

Endoplasmic reticulum stress refers to a cellular condition marked by the disruption of endoplasmic reticulum homeostasis due to increased protein synthesis, accumulation of misfolded proteins, or imbalanced calcium or redox levels (Ron & Walter, 2007). There are three major cellular signaling pathways designed to deal with this stress condition, initiated by three endoplasmic reticulum-located transmembrane molecules: PERK, IRE1, and ATF6 (Almanza *et al*, 2019). Enhanced activation of PERK and IRE1, but not ATF6, pathways was observed in TRAPPC1-deleted CMPs via mRNA and protein levels, indicating the potential involvement of PERK and IRE1 in TRAPPC1-deleted CMPs. The irreparable endoplasmic reticulum stress caused by TRAPPC1 deletion led to increased apoptosis and cell cycle arrest of CMPs. Importantly, the endoplasmic reticulum stress inhibitor TUDCA (Xie *et al*, 2002) significantly rescued the elevated apoptosis of TRAPPC1-deleted CMPs *in vitro*. Similarly, the PERK inhibitor GSK2606414 significantly rescued the defective proliferation of TRAPPC1-deleted CMPs. Apart from the elevated apoptosis of TRAPPC1-deleted CMPs, we also observed decreased autophagy of TRAPPC1-deleted CMPs compared with WT CMPs, consistent with a previous yeast study showing that TRAPP complex III promotes autophagy (Lynch-Day *et al*, 2010). Expression of the cyclin-dependent kinase inhibitor gene *cdkn1a* (p21) was elevated in TRAPPC1-deleted CMPs, as was the prevalence of p21-mediated cell senescence. These results collectively indicate that TRAPPC1 deficiency impairs CMPs through multiple pathways, including

endoplasmic reticulum stress, cell cycle arrest, senescence, and apoptosis.

As previously reported (Bassik *et al.*, 2013; Zhao *et al.*, 2017), the protein products of genes in the mammalian TRAPP family can be divided into two related complexes: TRAPP II and TRAPP III. Our gel filtration results offer the first piece of evidence indicating that TRAPPC1 plays a stabilizing role, at least partially, in mammalian cells. We observed similar changes to development ability and gene expression in TRAPPC3- and TRAPPC9-deficient CMPs, potentially suggesting that the indispensability of TRAPPC1 during myeloid cell development is more likely related to TRAPP complexes. However, as a commercial antibody against mouse TRAPPC1 has been previously unavailable and antihuman TRAPPC1 fails to cross-react with mouse TRAPPC1, we are unable to directly determine whether TRAPPC1 functions in primary mouse CMPs in its monomer form or as a complex, and this issue needs to be clarified in the future.

TRAPPC1 germline knockout mice were unattainable, likely due to fetal lethality, indicating a critical role for TRAPPC1 in fetal development and supporting our finding that TRAPPC1 deficiency tends to induce apoptosis in cells with high proliferative activity, as cell proliferation is one of the most important aspects of embryonic development. This might be one reason that no TRAPPC1 DNA variant-related diseases have been identified in humans to date (Sacher *et al.*, 2019).

Nevertheless, TRAPPC1 is indispensable for myeloid cell development, particularly for CMPs. TRAPPC1 deficiency leads to irreparable endoplasmic reticulum stress in CMPs, which subsequently induces apoptosis via a Ca²⁺ mitochondria-dependent pathway, as well as cell cycle arrest and senescence via the PERK/p21 pathway. This study highlights the vital role of TRAPPC1 in CMP maintenance and differentiation in mice.

Materials and Methods

Mice

CD45.1⁺ C57BL/6 mice were purchased from the Beijing Laboratory Animal Research Center (Beijing, China). ER^{Cre}-TRAPPC1^{loxp/loxp} (ER-TRAPPC1 KO) mice with C57BL/6 genetic background were obtained by crossing TRAPPC1^{loxp/loxp} mice with tamoxifen-inducible Cre mice (ER^{Cre} mice). ER^{Cre} mice and Lyz^{Cre} mice were kindly offered by Dr. Lianfeng Zhang (Key Laboratory of Human Diseases Comparative Medicine, Institute of Laboratory Animal Science). All mice were housed in specific pathogen-free conditions, and experiments described were carried out under the approval of the Institutional Animal Care and Use Committee of the Institute of Zoology (Beijing, China).

Reagents

The following antibodies were used: anti-mouse CD117 (2B8; 105825; Biolegend); anti-mouse CD16/32 (93; 12-0161-82; eBioscience); anti-mouse Sca-1 (D7; 108109; Biolegend); anti-mouse CD34 (SA376A4; 152205; Biolegend); Biotin Mouse Lineage Panel (559971; BD Bioscience); anti-mouse CD48 (HM48-1; 17-0481-82; eBioscience); anti-mouse CD150 (TC15-12F12.2; 115904; Biolegend); anti-mouse CD11b (M1/70; 101263; Biolegend); anti-mouse CD115 (AFS98; 135524; Biolegend); anti-mouse Ly6C (RB6-

8C5; 108406; Biolegend); anti-mouse Ly6G (1A8; 127606; Biolegend); anti-mouse CD4 (GK1.5; 100413; Biolegend); anti-mouse CD8a (53-6.7; 100738; Biolegend); anti-mouse B220 (RA3-6B2; 103224; Biolegend); anti-mouse CD45.1 (A20; 25-0453-82; eBioscience); anti-mouse CD45.2 (104; 109814; Biolegend); anti-mouse p21 (ab227443; abcam); anti-mouse ATF6 (ab37149; abcam); anti-mouse CHOP (L63F7; 2895 S; Cell Signaling Technology); anti-mouse Phospho-PERK (Thr982) (PA5-40294; eBioscience); anti-mouse Phospho-IRE1 (Ser724) (DF8322; Affinity Biosciences); anti-mouse XBP-1 S (Q3-695; 562642; BD Bioscience); anti-mouse Cytochrome c (6H2.B4; 612310; Biolegend); anti-ERGIC-53/p58 (E1031, Sigma); anti-GM130 (610822, BD Bioscience); Anti-TRAPPC4 (C-7, sc-390551, Santa Cruz); TRAPPC9, NIBP antibody (16014-1-AP, Proteintech); TRAPPC11 antibody (orb186301, Biorbyt). Other reagents included: Transcription Factor Phospho Buffer Set (565575; BD Bioscience); Active Caspase-3 Apoptosis Kit (550914; BD Bioscience); 647 EdU Click Proliferation Kit (565456; BD Bioscience); Mitochondrial membrane potential assay kit with JC-1 (C2006; Beyotime); Total Reactive Oxygen Species (ROS) Assay Kit (88-5930-74, Thermo Fisher); CYTO-ID Autophagy detection kit (ENZ-51031; Enzo Biochem); Senescence β -Galactosidase Staining Kit (C0602; Beyotime); BCA Protein Assay Kit (P0011, Beyotime); Tauroursodeoxycholic Acid (TUDCA) (S3654; Selleck); Tamoxifen (T5648; Sigma); GSK2606414 (S7307; Selleck); Thapsigargin (T9033; Sigma), Gel Filtration Standard (1511901, Bio-Rad).

Bone marrow chimeras

Recipient CD45.1⁺ mice were irradiated twice with 4.5 Gy (9 Gy total) at 3-h intervals. For complete chimeras, 5 × 10⁶ bone marrow cells (BMCs) from CD45.2⁺ WT or CD45.2⁺ ER-TRAPPC1 mice were transferred intravenously 3 h after irradiation (Liu *et al.*, 2013). For mixed chimeras, BMCs from CD45.1⁺CD45.2⁺ WT and CD45.2⁺ ER-TRAPPC1 mice were mixed at a ratio of 1:1, after which 5 × 10⁶ mixed cells were transferred intravenously. Reconstitution of chimeras was analyzed at 6–8 weeks for quality assurance.

Adoptive transfer of myeloid progenitors

Sorted myeloid progenitors (Lin⁻Sca1⁻CD117⁺) from CD45.2⁺ WT or CD45.2⁺ ER-TRAPPC1 mice treated with tamoxifen for three consecutive days *in vivo* were transferred intravenously into CD45.1⁺CD45.2⁺ recipient mice, which were pretreated with 3 Gy irradiation. Recipients were tested 6 days after transplantation.

Methylcellulose colony-forming assays

Sorted CMPs (Lin⁻Sca1⁻CD117⁺CD16/32^{low}CD34⁺) were placed in MethoCult M3134 supplemented with 50 ng/ml SCF, 10 ng/ml IL-6, 10 ng/ml IL-3, 10 μ g/ml insulin, 20 ng/ml M-CSF, or 20 ng/ml G-CSF, as described previously (Zhao *et al.*, 2018). Approximately 5,000 cells were plated on each 35 mm dish, and colonies were counted and analyzed after 5–7 days of culturing as described.

Flow cytometry analysis and sorting

Cells were stained with fluorescein-conjugated antibodies in PBS containing 0.1% BSA and 0.1% NaN₃ at 4°C for 30 min in dark.

Stained samples were then analyzed by Gallios Flow Cytometer (Beckman Coulter) and BD LSRFortessa™ X-20 (Becton Dickinson) or sorted using a MoFlo Astrios EQ Cell Sorter (Beckman Coulter). Flow cytometry data were analyzed by FCS Express (*De Novo* Software) and FlowJo software (TreeStar).

Transmission electron microscopy

CMP cells were sorted by a fluorescence-activated cell sorter and directly collected into Phosphate Buffer Saline (PBS) containing glutaraldehyde (with a final concentration of 2.5%) for real-time fixation. Four hours after fixing, the cells were embedded in 3% agar, followed by multistep cutting and staining processes. Images were acquired on a Tecnai G2 F20 electron microscope equipped with a ZrO₂/W (100) Schottky Field emitter source and operating at 120 kV.

Immunofluorescence staining

Sorted cells were incubated overnight in Poly-D-Lysine-coated 35 mm dishes with complete medium containing 10% FBS to allow cell adhesion. Cells were then fixed in 4% paraformaldehyde and permeabilized in 0.3% Triton X-100/PBS for 10 min at 4°C. Cells were blocked for 1 h in PBS containing 1% BSA and 0.3% Triton X-100, then incubated with primary antibodies overnight at 4°C. For endoplasmic reticulum and Golgi apparatus labeling, cells were incubated with fluorescein-conjugated lectins for 2 h. After PBS washing, cells were labeled by incubation with secondary antibodies for 2 h, then stained with Hoechst 33342 (4 µg/ml) for 10 min. Photomicrographs were taken using an Andor Dragonfly high speed confocal (Andor Technology Ltd, Belfast UK).

5-ethynyl-2'-deoxyuridine (EdU) incorporation assay

Mice were treated with tamoxifen as described above. Twelve hours before sacrificing, mice were intravenously injected with 1 mg of 5-ethynyl-2'-deoxyuridine (EdU) dissolved in PBS. Bone marrow cells were harvested as described above, and EdU incorporation was assessed using an EdU Click Proliferation Kit (BD Bioscience) and analyzed on a BD LSRFortessa™ X-20 (Becton Dickinson) via flow cytometry.

Ca²⁺ measurement

Cytosolic Ca²⁺ was measured using Fluo-4 AM (Beyotime), and mitochondrial Ca²⁺ was measured using Rhod-2 AM (AAT Bioquest), both according to the manufacturers' instructions. Briefly, after labeling with antibodies specific for precursor makers, bone marrow cells were suspended and incubated with 1 µM of Fluo-4 AM or 1 µM of Rhod-2 AM in PBS at 37°C for 30 min, then washed three times with PBS. Samples were allowed to stand for at least 15 min between the final wash and analysis to allow the dye de-esterification process to complete. Fluorescent intensity was detected in the FITC channel (for Fluo-4) or PE channel (for Rhod-2) with flow cytometry.

Detection of mitochondrial membrane potential

Mitochondrial membrane potential detection was performed by staining cells with JC-1 (Beyotime) according to the manufacturers'

instructions. In detail, bone marrow cells were first labeled with antibodies specific to precursor makers, as mentioned above. After washing away free antibodies with PBS, cells were loaded with JC-1 for 25 min at 37°C, then rinsed three times. During flow cytometry analysis, JC-1 aggregates with red fluorescence were detected in the PE channel (excitation at 561 nm and emission at 586 ± 15 nm), whereas monomers with green fluorescence were detected in the FITC channel (excitation at 488 nm and emission at 530 ± 15 nm).

Cytochrome c leaking out experiment

For intracellular cytochrome C staining, bone marrow cells were first treated on ice for 8 min with either control or 6 µg/ml digitonin, then washed twice with PBS and labeled with antibodies specific for precursor markers, as described above. Cells were then fixed and permeated with BM Cytifix Buffer sets (BD Biosciences) and stained with anti-cytochrome C (clone: 6H2.B4, conjugated with Alexa Fluor® 647).

Gel filtration

CMPs from WT and ER-TRAPPC1 KO mice were sorted and homogenized in buffer (150 mM NaCl, 20 mM HEPES, 2 mM EDTA, 1 mM DTT and Protease inhibitor, pH 7.2). Protein samples were loaded onto a Superose6 gel filtration column (GE), and 3-ml fractions were collected and concentrated with an ultrafiltration tube. Concentrated proteins were detected by western blot using specific antibodies.

Senescence β-Galactosidase staining

Sorted CMPs were washed with PBS and stained with a Senescence β-Galactosidase Staining kit according to manufacturers' instructions. Stained cells were viewed and imaged under a light microscope.

Gene knockdown with small interference RNA

Sorted CMPs were treated with si-RNAs targeting TRAPPC3 and TRAPPC9 using electroporation (sequences listed in Appendix Table S2). Cells were then cultured with SCF (20 ng/ml), GM-CSF (10 ng/ml), G-CSF (20 ng/ml), and M-CSF (20 ng/ml) for 5–7 days and detected as described.

RNA extraction and quantitative PCR analysis

Total RNA was extracted using a MicroElute Total RNA Kit (R6831) according to the product manufacturer's instructions. Reverse transcription was performed with M-MLV superscript reverse transcriptase. Quantitative real-time PCR was performed using SYBR kits (SYBR Premix Ex Taq, DRR041A, Takara Bio) on an CFX96 (Bio-Rad) real-time PCR machine (Chu *et al.*, 2020). All gene expression levels reported in this study were normalized using the housekeeping gene hypoxanthine phosphoribosyl transferase (HPRT). Target genes and primer sequences are shown in Appendix Table S1.

RNA sequencing analysis

Total RNA was extracted from sorted CMPs and GMPs using TRIzol Reagent, and sequencing library generation and processing were

performed by Novogene Company. The R package DESeq v1.32.052 was used to compare gene expression profiles, and differentially expressed genes (DEGs) were further analyzed by Kyoto Encyclopedia of Genes and Genomes (KEGG) pathway analysis and Gene Ontology analysis.

Statistical analysis

All data are shown as mean \pm SD. Statistical significance was determined with the two-tailed student's *t*-test.

Data availability

The data sets produced in this study are available in the following databases: RNA-Seq data: Gene Expression Omnibus GSE201077 (<https://www.ncbi.nlm.nih.gov/geo/query/acc.cgi?acc=GSE201077>).

Expanded View for this article is available [online](#).

Acknowledgments

The authors thank Dr. Yangxiao Hou and Dr. Qianchuan Tian for their critical review of our manuscript, Ms. Qing Meng, Ms. Guoli Hou, Mr. Pengyan Xia, and Ms. Xiaoqiu Liu for their expert technical assistance, Ling Li for her excellent laboratory management, and Peng Zhang for his outstanding animal husbandry. This work was supported by grants from the National Natural Science Foundation for Key Programs (31930041, Y.Z.), the National Key Research and Development Program of China (2017YFA0105002, 2017YFA0104402, Y.Z.), and the Knowledge Innovation Program of the Chinese Academy of Sciences (XDA16030301, Y.Z.).

Author contributions

Yanan Xu: Conceptualization; formal analysis; validation; investigation; visualization; writing—original draft; writing—review and editing. **Zhaoqi Zhang:** Software; visualization; methodology; writing—original draft; writing—review and editing. **Yang Zhao:** Formal analysis; investigation; methodology; writing—original draft; writing—review and editing. **Chenxu Zhao:** Validation; visualization; methodology. **Mingpu Shi:** Data curation; formal analysis; validation. **Xue Dong:** Data curation; formal analysis; validation. **Jiayu Zhang:** Data curation; formal analysis. **Liang Tan:** Formal analysis; methodology. **Lianfeng Zhang:** Resources; supervision; writing—original draft; project administration; writing—review and editing. **Yong Zhao:** Supervision; funding acquisition; writing—original draft; project administration; writing—review and editing.

Disclosure and competing interests statement

The authors declare no conflicts of actual or perceived competing interests.

References

- Almanza A, Carlesso A, Chinthra C, Creedican S, Doultosinos D, Leuzzi B, Luis A, McCarthy N, Montibeller L, More S *et al* (2019) Endoplasmic reticulum stress signalling - from basic mechanisms to clinical applications. *FEBS J* 286: 241–278
- Alvarez-Errico D, Vento-Tormo R, Sieweke M, Ballestar E (2015) Epigenetic control of myeloid cell differentiation, identity and function. *Nat Rev Immunol* 15: 7–17
- Bahar E, Kim H, Yoon H (2016) ER stress-mediated signaling: Action potential and Ca²⁺ as key players. *Int J Mol Sci* 17: 1558
- Barlowe CK, Miller EA (2013) Secretory protein biogenesis and traffic in the early secretory pathway. *Genetics* 193: 383–410
- Bassik MC, Kampmann M, Lebbink RJ, Wang S, Hein MY, Poser I, Weibezahn J, Horlbeck MA, Chen S, Mann M *et al* (2013) A systematic mammalian genetic interaction map reveals pathways underlying ricin susceptibility. *Cell* 152: 909–922
- Bodnar B, DeGruttola A, Zhu Y, Lin Y, Zhang Y, Mo X, Hu W (2020) Emerging role of NIK/IKK2-binding protein (NIBP)/trafficking protein particle complex 9 (TRAPPC9) in nervous system diseases. *Transl Res* 224: 55–70
- Cejas RB, Tamano-Blanco M, Blanco JG (2021) Analysis of the intracellular traffic of IgG in the context of down syndrome (trisomy 21). *Sci Rep* 11: 10981
- Chen X, Zhang W, Gao YF, Su XQ, Zhai ZH (2002) Senescence-like changes induced by expression of p21(waf1/Cip1) in NIH3T3 cell line. *Cell Res* 12: 229–233
- Chu Z, Sun C, Sun L, Feng C, Yang F, Xu Y, Zhao Y (2020) Primed macrophages directly and specifically reject allografts. *Cell Mol Immunol* 17: 237–246
- Clausen BE, Burkhardt C, Reith W, Renkawitz R, Forster I (1999) Conditional gene targeting in macrophages and granulocytes using LysMcre mice. *Transgenic Res* 8: 265–277
- Dang EV, McDonald JG, Russell DW, Cyster JG (2017) Oxysterol restraint of cholesterol synthesis prevents AIM2 Inflammasome activation. *Cell* 171: 1057–1071.e11
- Dong X, Liang Z, Zhang J, Zhang Q, Xu Y, Zhang Z, Zhang L, Zhang B, Zhao Y (2022) Trappc1 deficiency impairs thymic epithelial cell development by breaking endoplasmic reticulum homeostasis. *Eur J Immunol* 52: 1789–1804
- Flodby P, Li C, Liu Y, Wang H, Marconett CN, Laird-Offringa IA, Minoo P, Lee AS, Zhou B (2016) The 78-kD glucose-regulated protein regulates endoplasmic reticulum homeostasis and distal epithelial cell survival during lung development. *Am J Respir Cell Mol Biol* 55: 135–149
- Gonzalez D, Espino J, Bejarano I, Lopez JJ, Rodriguez AB, Pariente JA (2010) Caspase-3 and -9 are activated in human myeloid HL-60 cells by calcium signal. *Mol Cell Biochem* 333: 151–157
- Hirsch I, Weiward M, Prell E, Ferrari DM (2014) ERp29 deficiency affects sensitivity to apoptosis via impairment of the ATF6-CHOP pathway of stress response. *Apoptosis* 19: 801–815
- Hsu CH, Altschuler SJ, Wu LF (2019) Patterns of early p21 dynamics determine proliferation-senescence cell fate after chemotherapy. *Cell* 178: 361–373.e12
- Iurlaro R, Munoz-Pinedo C (2016) Cell death induced by endoplasmic reticulum stress. *FEBS J* 283: 2640–2652
- Iwasaki H, Akashi K (2007) Myeloid lineage commitment from the hematopoietic stem cell. *Immunity* 26: 726–740
- Jeong M, Sun D, Luo M, Huang Y, Challen GA, Rodriguez B, Zhang X, Chavez L, Wang H, Hannah R *et al* (2014) Large conserved domains of low DNA methylation maintained by Dnmt3a. *Nat Genet* 46: 17–23
- Kamiya T, Watanabe M, Hara H, Mitsugi Y, Yamaguchi E, Itoh A, Adachi T (2018) Induction of human-lung-cancer-A549-cell apoptosis by 4-Hydroperoxy-2-decanoic acid ethyl ester through intracellular ROS accumulation and the induction of proapoptotic CHOP expression. *J Agric Food Chem* 66: 10741–10747
- Karmaus PWF, Herrada AA, Guy C, Neale G, Dhungana Y, Long L, Vogel P, Avila J, Clish CB, Chi H (2017) Critical roles of mTORC1 signaling and metabolic reprogramming for M-CSF-mediated myelopoiesis. *J Exp Med* 214: 2629–2647

- Kim JJ, Lipatova Z, Segev N (2016) TRAPP complexes in secretion and autophagy. *Front Cell Dev Biol* 4: 20
- Krebs J, Agellon LB, Michalak M (2015) Ca(2+) homeostasis and endoplasmic reticulum (ER) stress: an integrated view of calcium signaling. *Biochem Biophys Res Commun* 460: 114–121
- Lee S, Lee KS, Huh S, Liu S, Lee DY, Hong SH, Yu K, Lu B (2016) Polo kinase phosphorylates Miro to control ER-mitochondria contact sites and mitochondrial Ca(2+) homeostasis in neural stem cell development. *Dev Cell* 37: 174–189
- Liu G, Hu X, Sun B, Yang T, Shi J, Zhang L, Zhao Y (2013) Phosphatase Wip1 negatively regulates neutrophil development through p38 MAPK-STAT1. *Blood* 121: 519–529
- Lynch-Day MA, Bhandari D, Menon S, Huang J, Cai H, Bartholomew CR, Brummell JH, Ferro-Novick S, Klionsky DJ (2010) Trs85 directs a Ypt1 GEF, TRAPPIII, to the phagophore to promote autophagy. *Proc Natl Acad Sci USA* 107: 7811–7816
- Mahalingaiah PK, Palenski T, Van Vleet TR (2018) An *in vitro* model of hematotoxicity: differentiation of bone marrow-derived stem/progenitor cells into hematopoietic lineages and evaluation of lineage-specific hematotoxicity. *Curr Protoc Toxicol* 76: e45
- Maurel M, McGrath EP, Mnich K, Healy S, Chevet E, Samali A (2015) Controlling the unfolded protein response-mediated life and death decisions in cancer. *Semin Cancer Biol* 33: 57–66
- Mihailidou C, Papazian I, Papavassiliou AG, Kiaris H (2010) CHOP-dependent regulation of p21/waf1 during ER stress. *Cell Physiol Biochem* 25: 761–766
- Mohamed E, Sierra RA, Trillo-Tinoco J, Cao Y, Innamarato P, Payne KK, de Mingo PA, Mandula J, Zhang S, Thevenot P et al (2020) The unfolded protein response mediator PERK governs myeloid cell-driven immunosuppression in tumors through inhibition of STING signaling. *Immunity* 52: 668–682
- Munoz JP, Ivanova S, Sanchez-Wandelmer J, Martinez-Cristobal P, Noguera E, Sancho A, Diaz-Ramos A, Hernandez-Alvarez MI, Sebastian D, Mauvezin C et al (2013) Mfn2 modulates the UPR and mitochondrial function via repression of PERK. *EMBO J* 32: 2348–2361
- Ramirez-Peinado S, Ignashkova TI, van Raam BJ, Baumann J, Sennott EL, Gendarme M, Lindemann RK, Starnbach MN, Reiling JH (2017) TRAPPC13 modulates autophagy and the response to Golgi stress. *J Cell Sci* 130: 2251–2265
- Rashid HO, Yadav RK, Kim HR, Chae HJ (2015) ER stress: autophagy induction, inhibition and selection. *Autophagy* 11: 1956–1977
- Ron D, Walter P (2007) Signal integration in the endoplasmic reticulum unfolded protein response. *Nat Rev Mol Cell Biol* 8: 519–529
- Rosenbauer F, Tenen DG (2007) Transcription factors in myeloid development: balancing differentiation with transformation. *Nat Rev Immunol* 7: 105–117
- Rozpedek W, Pytel D, Mucha B, Leszczynska H, Diehl JA, Majsterek I (2016) The role of the PERK/elf2alpha/ATF4/CHOP signaling pathway in tumor progression during endoplasmic reticulum stress. *Curr Mol Med* 16: 533–544
- Sacher M, Jiang Y, Barrowman J, Scarpa A, Burston J, Zhang L, Schieltz D, Yates JR 3rd, Abeliovich H, Ferro-Novick S (1998) TRAPP, a highly conserved novel complex on the cis-Golgi that mediates vesicle docking and fusion. *EMBO J* 17: 2494–2503
- Sacher M, Barrowman J, Wang W, Horecka J, Zhang Y, Pypaert M, Ferro-Novick S (2001) TRAPP I implicated in the specificity of tethering in ER-to-Golgi transport. *Mol Cell* 7: 433–442
- Sacher M, Shahrzad N, Kamel H, Milev MP (2019) TRAPPopathies: an emerging set of disorders linked to variations in the genes encoding transport protein particle (TRAPP)-associated proteins. *Traffic* 20: 5–26
- Schwarz DS, Blower MD (2016) The endoplasmic reticulum: structure, function and response to cellular signaling. *Cell Mol Life Sci* 73: 79–94
- Scrivens PJ, Noueihed B, Shahrzad N, Hul S, Brunet S, Sacher M (2011) C4orf41 and TTC-15 are mammalian TRAPP components with a role at an early stage in ER-to-Golgi trafficking. *Mol Biol Cell* 22: 2083–2093
- Shahrin NH, Diakiw S, Dent LA, Brown AL, D'Andrea RJ (2016) Conditional knockout mice demonstrate function of Klf5 as a myeloid transcription factor. *Blood* 128: 55–59
- Shen M, Wang L, Wang B, Wang T, Yang G, Shen L, Wang T, Guo X, Liu Y, Xia Y et al (2014) Activation of volume-sensitive outwardly rectifying chloride channel by ROS contributes to ER stress and cardiac contractile dysfunction: involvement of CHOP through Wnt. *Cell Death Dis* 5: e1528
- Sun D, Luo M, Jeong M, Rodriguez B, Xia Z, Hannah R, Wang H, Le T, Faull KF, Chen R et al (2014) Epigenomic profiling of young and aged HSCs reveals concerted changes during aging that reinforce self-renewal. *Cell Stem Cell* 14: 673–688
- Taiwo O, Wilson GA, Emmett W, Morris T, Bonnet D, Schuster E, Adejumo T, Beck S, Pearce DJ (2013) DNA methylation analysis of murine hematopoietic side population cells during aging. *Epigenetics* 8: 1114–1122
- Tam AB, Roberts LS, Chandra V, Rivera IG, Nomura DK, Forbes DJ, Niwa M (2018) The UPR activator ATF6 responds to proteotoxic and lipotoxic stress by distinct mechanisms. *Dev Cell* 46: 327–343.e7
- Wang L, Liu H, Zhang X, Song E, Wang Y, Xu T, Li Z (2021) WFS1 functions in ER export of vesicular cargo proteins in pancreatic beta-cells. *Nat Commun* 12: 6996
- Xie Q, Khaoustov VI, Chung CC, Sohn J, Krishnan B, Lewis DE, Yoffe B (2002) Effect of tauroursodeoxycholic acid on endoplasmic reticulum stress-induced caspase-12 activation. *Hepatology* 36: 592–601
- Xu L, Liu X, Peng F, Zhang W, Zheng L, Ding Y, Gu T, Lv K, Wang J, Ortinau L et al (2020) Protein quality control through endoplasmic reticulum-associated degradation maintains haematopoietic stem cell identity and niche interactions. *Nat Cell Biol* 22: 1162–1169
- Yamasaki A, Menon S, Yu S, Barrowman J, Meerloo T, Oorschot V, Klumperman J, Satoh A, Ferro-Novick S (2009) mTrs130 is a component of a mammalian TRAPP II complex, a Rab1 GEF that binds to COPI-coated vesicles. *Mol Biol Cell* 20: 4205–4215
- Yu IM, Hughson FM (2010) Tethering factors as organizers of intracellular vesicular traffic. *Annu Rev Cell Dev Biol* 26: 137–156
- Zhang DE, Zhang P, Wang ND, Hetherington CJ, Darlington GJ, Tenen DG (1997) Absence of granulocyte colony-stimulating factor signaling and neutrophil development in CCAAT enhancer binding protein alpha-deficient mice. *Proc Natl Acad Sci USA* 94: 569–574
- Zhao S, Li CM, Luo XM, Siu GK, Gan WJ, Zhang L, Wu WK, Chan HC, Yu S (2017) Mammalian TRAPPIII complex positively modulates the recruitment of Sec13/31 onto COPII vesicles. *Sci Rep* 7: 43207
- Zhao Y, Shen X, Na N, Chu Z, Su H, Chao S, Shi L, Xu Y, Zhang L, Shi B et al (2018) mTOR masters monocyte development in bone marrow by decreasing the inhibition of STAT5 on IRF8. *Blood* 131: 1587–1599